

# THE UTILIZATION OF SYNTHESIZED COHERENCE FUNCTION IN OPTICAL TIME-DOMAIN REFLECTOMETRY

Jozef Jasenek \*

The paper deals with the synthesis of an optical coherence function and its application in Optical Time-Domain Reflectometry (OTDR). A brief summary of up-to-date approaches to the optical reflectometry is given. The fundamental equation of Optical Coherence-Domain Reflectometry with Synthesized Coherence Function (OCDR-SCF) is derived and a general theoretical approach to the synthesis of a coherence function of arbitrary shape is outlined. The obtained results are illustrated on the synthesis of three different shapes of coherence function. The main performance parameters of the OCDR-SCF and the most significant advantages and drawbacks of this approach are discussed.

**Keywords:** Coherence function, OTDR, diagnostics of optical systems and components

## 1 INTRODUCTION

OTDR is today a well-established tool for non-destructive characterization of fiber optic components and networks. Generally, an ideal reflectometry system should have a sufficient spatial resolution to clearly indicate the closely separated sites of reflections within the tested network or device. Moreover, the system should have a good sensitivity to be able to detect very low power signals originating from the Rayleigh back scattering and simultaneously a relatively high dynamical range to process rather high power levels coming from discrete Fresnel reflections.

In the original OTDR [1] in which systems are probed with rather short pulses of high power level optical radiation there is a trade-off between the space resolution and dynamical range. The spatial resolution is improved when the pulses are getting shorter and the measurement bandwidth is increased. This raises the noise levels detected and results in dynamical range reduction. Moreover, the shortening of the probe impulse means a decrease of energy available for detection. To solve these problems a number of new techniques and approaches were suggested and investigated since the time of invention of OTDR by Barnoski and Jensen in 1976. As an example we can mention here quickly the correlation OTDR based on the use of a pseudorandom signal [2] or signal modulated by complementary Golay code [3], coherent OTDR [4], photon-counting OTDR [5], low correlation OTDR [6], frequency-domain optical reflectometry (OFDR) with the linear frequency scanning [7] or with frequency modulation of the intensity [8]. The most significant and innovative contribution to these new techniques is the so-called optical coherence-domain reflectometry with a synthesized coherence function (OCDR-SCF) [9]. It does not utilize any mechanical moving parts and obtaining of the measurement results is straightforward without any calculation.

The goal of this contribution is a detailed analysis of the OCDR-SCF and investigation of the procedure for the synthesis of the coherence function (CF) with an arbitrary shape. Finally, the main performance parameters, advantages and drawbacks of this method are discussed.

## 2 THE PRINCIPLE OF OCDR-SCF

The basic idea of the OCDR-SCF can be explained using the simplified block diagram of the optical reflectometer based on this method that is drawn in the Fig. 1.

It is a properly Michelson interferometer driven by an optical highly coherent laser tunable in a relatively broad frequency range. The acousto-optical deflector shifts up the oscillation frequency  $\omega_0$  of the deviated beam by  $\omega$ . The phase modulator P-MOD allows to change continually the phase of the optical wave in the reference arm in the range of  $\pm\pi$ . Signals coming from the reference arm and the measuring one are combined at the 3 dB beam splitter OBS-2. The two splitted signals leaving the OBS-2 are the same but mutually shifted in phase by  $\pi$ , which allows for excluding the influence of the noise. The optical signal incident on the photo-detector PD-1 can be described by the expression in the complex form

$$E(t) = E_0 e^{j[(\omega_0 - \omega)t + \varphi(t)]} + E_0 \int_0^L \rho(z) \delta n(z) e^{j[\omega_0(t) + \varphi(t - (2z/v_g))]} \cdot e^{-jk_2 z} dz. \quad (1)$$

The first and second terms in (1) represent the signals from the reference and measuring arms, respectively. The second term describes the superposition of signals back-scattered from the particular elementary sections  $dz$  distributed along the DUT [10], see Fig. 1. It is to be stressed

\* Slovak University of Technology, Faculty of Electrical Engineering and Information Technology, Department of Electromagnetic Theory, Ilkovičova 3, 812 19 Bratislava 1, Slovakia, e-mail: Jozef.Jasenek@elf.stuba.sk

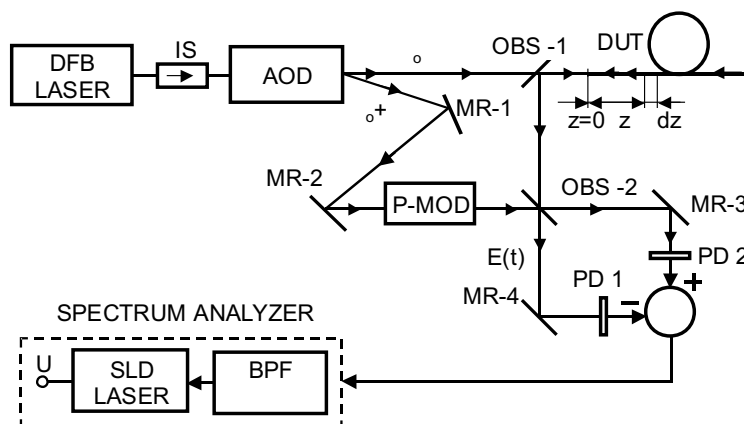


**Fig. 1.** Simplified block diagram of the optical reflectometer based on OADR-SCF. IS — optical isolator, AOD — acusto-optic deflector, OBS-1,2 — optical beam-splitters, DUT — device under test, MR-1-4 — mirrors, PD1,2 — photodetectors, P-MOD — phase modulator, BPF — band pass filter, SLD — square-law detector.

that the amplitudes of these signals are directly proportional to the local reflection coefficient  $\rho(z)$  and local fluctuation of the refractive index  $\delta n(z)$ .  $E_0$  and  $\omega_0$  are the amplitude and central oscillation frequency of the optical source respectively.  $\varphi(t)$  is random function describing the phase fluctuation of the optical source.  $v_g$  and  $k$  are the group velocity and the wave number in the tested wave-guide, respectively.

The output signal from the balanced photo-detector goes through the band-pass filter. Only intermediate frequency component is selected from the mixing product at the detector. The average value of the intermediate frequency signal at the output of the balanced photo-detector can be described by

$$i(t) = \text{Re} \left\{ K \cdot E_0^2 \cdot e^{j\omega t} \cdot \int_0^L \rho(z) \delta n(z) \left[ \frac{1}{T} \cdot \int_0^T e^{j[\varphi(t-(2z/v_g)) - \varphi(t)]} dt \right] \cdot e^{-jk2z} dz \right\} \quad (2)$$

where  $K$  is a proportionality constant.

The averaging concerns the phase fluctuations of the optical source, which are characterized by their spectral power density. The inner time integral in (2) defines the coherence function  $\gamma(z)$  of the optical source. It is generally known that the Fourier transform of the coherence function defines the spectral power density of the source [11]. Hence the power spectrum shape is closely related to the coherence function. Consequently, *to synthesize a suitable coherence function means to create the corresponding time average spectrum shape*. The possibilities for the shaping of the average optical spectrum will dominantly restrict the synthesis of a required coherence function.

The back-scattered signal is of random nature not only due to the random phase fluctuation in time but also to the random microscopic fluctuations of the refraction index along the tested device. To process these fluctuations

it is necessary to use a square-law detector. Its output signal is sensitive to the correlation function  $\langle \delta n(z_1) \delta n(z_2) \rangle$ . The signal  $U$  at the output of the square-law detector is given by the integral

$$U \approx E_0^4 \int_0^L \int_0^L \rho(z_1) \rho(z_2) \gamma(z_1) \gamma(z_2) \langle \delta n(z_1) \delta n(z_2) \rangle \cdot e^{-j2k(z_1+z_2)} dz_1 dz_2. \quad (3)$$

Taking into account that the correlation function  $\langle \delta n(z_1) \delta n(z_2) \rangle$  in glass can be roughly approximated by the  $\delta(z_1 - z_2)$  function [12], integral (3) can be then rewritten into the form

$$U \approx E_0^4 \int_0^L |\rho(z)|^2 |\gamma(z)|^2 dz. \quad (4)$$

This integral offers a very interesting suggestion. If the absolute value of the coherence function  $\gamma(z)$  could be made similar to the  $\delta(z)$ -like shape then the output signal of the square-law detector would be directly proportional to the squared absolute value of the reflection coefficient to be measured.

$$U \approx E_0^4 |\rho(z)|^2. \quad (5)$$

From the experimental point of view (5) represents a very interesting and significant result. Using of the  $\delta$ -like SCF allows a direct measurement of the space distribution of reflection coefficient along the DUT without the need for any lengthy calculation as it is the case at other methods.

In the following section we demonstrate the possibility of realization of such a coherence function.

### 3 THE SYNTHESIS OF THE COHERENCE FUNCTION

Let us consider first an ideal monochromatic laser diode with central oscillation frequency  $\omega_0$  and with no

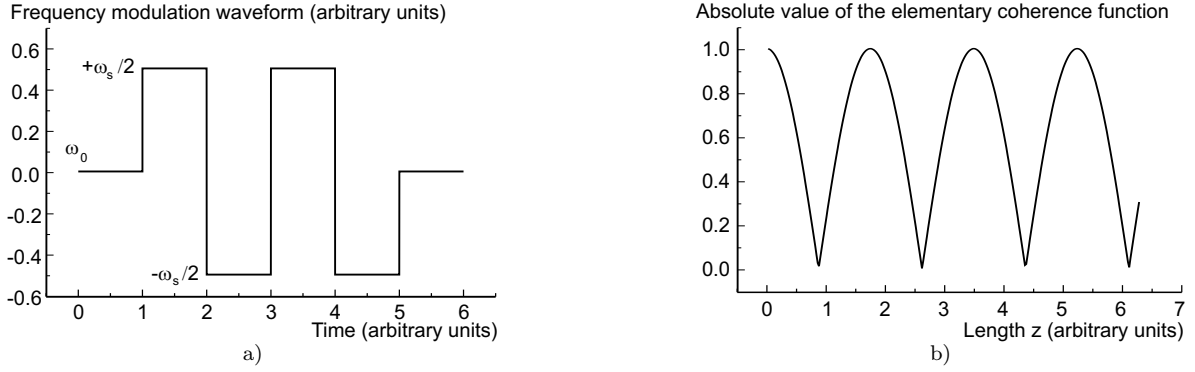


**Fig. 2.** Frequency modulation (a) and absolute value of the “elementary” synthesized coherence function (b).

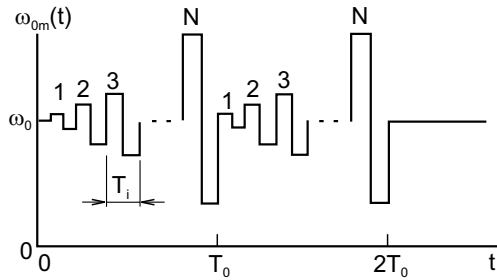


**Fig. 3.** The stepwise modulation of the source frequency,  $T_i$  — duration of  $i$ -th step in modulation waveform,  $T_0$  — the period of the modulation waveform,  $N$  — the number of steps in the modulation waveform.

phase fluctuations  $\varphi(t)$  launched into the interferometer, see relation (2) and Fig. 1. The injection current of the diode is modulated by a periodical and symmetrical square waveform. It is proposed that also the frequency of the diode is modulated by the same waveform. The laser frequency will be switching between two values  $\omega_0 - \omega_s/2$  and  $\omega_0 + \omega_s/2$ , where  $\omega_s$  is the absolute change of the angular frequency (separation frequency) during one period of the modulation waveform, see Fig. 2. It can be easily shown that the coherence function of this periodically modulated optical wave can be found according to relation (2) in the form

$$\gamma(\tau) = \cos \frac{\omega_s}{2} \tau \quad (6)$$

where  $\tau = 2z/v_g$  is the round trip optical time delay between the reference and scattered signals, see Fig. 2.  $k = k(t)$  is the wave number in the DUT that changes in time similarly as the modulation waveform.

This result suggests the possibility to generate a set of similar function with frequencies which are integer multiples of  $\omega_s$ , through a suitable modulation of the laser frequency. Superposition of these partial coherence functions may be used for the synthesis of an arbitrary shape periodic coherence function. Let us consider now the stepwise shape of the laser diode modulation current. The frequency response to this current, which is expected to be directly proportional to the modulation current, is

outlined in Fig. 3. In each following step of the modulation waveform the frequency change increases by  $\omega_s$ . The maximum frequency change  $N\omega_s$  takes place in the last step of the waveform. According to the result obtained above each modulation step gives one term of the intended SCF. The whole modulation waveform produces a set of elementary CFs described by (7). It is important to note that the generation of these CFs is obtained through the process of subsequent time averaging running through all steps of the whole modulation waveform.

$$\begin{aligned} \cos(\omega_s \cdot z/v_g), \cos(2\omega_s \cdot z/v_g), \cos(3\omega_s \cdot z/v_g), \\ \cos(4\omega_s \cdot z/v_g), \dots, \cos(N\omega_s \cdot z/v_g) \quad (7) \end{aligned}$$

If there were some possibility to adjust the initial phases of the particular terms in (7), they could be used in a similar way as it is done in the theory of Fourier series. Such a phase shift can be realized by the phase modulator driven synchronously by the modulation signal that is proportional to the one used for frequency modulation. The modulator can be placed in one of the arms of the interferometer, see Fig. 1. As a result the functions (7) take the form

$$\begin{aligned} \cos[\omega_s/v_g(z - z\zeta)], \cos[2\omega_s/v_g(z - z\zeta)], \cos[3\omega_s/v_g(z - z\zeta)], \\ \cos[4\omega_s/v_g(z - z\zeta)], \dots, \cos[N\omega_s/v_g(z - z\zeta)] \quad (8) \end{aligned}$$

In order to be able to synthesize the periodic CF of arbitrary form, like as it is in the Fourier series, it is necessary to have the possibility to realize also proper multiplication coefficients for each term in (8). It can be achieved by a proper adjusting of the duration of each step in the frequency and also in the phase modulation waveforms. As it will be shown later, the duration of each step will determine the amplitude of the particular term in the SCF. In this way the modulation waveforms will become more complicated and more difficult to realize [13].

In the following, using the method described above, we shall try to illustrate how one can synthesize the coherence function of the  $\delta$ -like, triangle and the square shape.

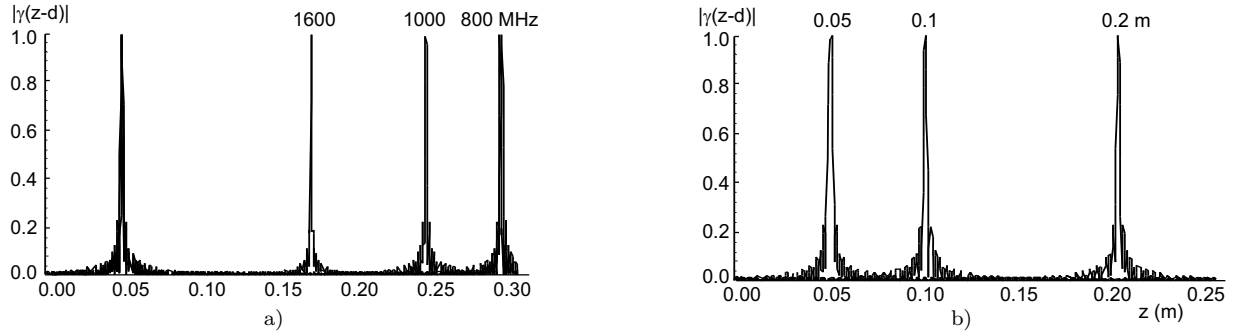


**Fig. 4.** The illustration of the  $\delta$ -like SCF and of the scanning of its peaks position — through the scanning of the separation frequency (shown for  $f_s = 800, 1000, 1600$  MHz) while the phase shift is constant  $z_\xi = 0.5$  m (a) and through the scanning of phase shift (shown first peak for  $z = 0.05, 0.1, 0.2$  m) while the separation frequency is constant  $f_s = 800$  MHz (b).

### 1. The synthesis of the $\delta$ -like coherence function

Let us consider an ideal monochromatic laser diode with central frequency  $\omega_0$  modulated by a suitable current wave form resulting in frequency modulation as outlined in Fig. 3. We will show that in this case the periodic  $\delta$ -like coherence function can be synthesized. However, it is possible only if the duration of any step in the modulation waveform is long enough as compared with the round trip time delay  $\tau = 2z/v_g$ . In order to get more general results let us consider first the frequency modulation waveform similar as outlined in Fig. 3, but the duration  $T_i$  of each symmetrical step in the waveform is proposed to be different for all of them. Following relation (2), the signal at the output of the photo-detector can be written in the form

$$i(t) \approx \int_0^L \rho(z) \left\{ \frac{1}{T_0} \int_0^{T_0} \exp\left\{j\left[\omega t - \omega_{om}(t') \frac{2z}{v_g}\right]\right\} dt' \right\} dz. \quad (9)$$

Here,  $\omega_{om}(t')$  is a function describing the time dependence of the frequency modulation waveform. It is given by

$$\omega_{om}(t') = \omega_0 + \alpha(t') \cdot \frac{\omega_0}{2}, \quad (10)$$

$\omega_0$  is the central oscillation frequency of the source and

$$\alpha(t') = \sum_{i=1}^N i \cdot \frac{\omega_s}{2} \left[ 1(t' - \sum_{k=0}^{i-1} T_k) - 2 \cdot 1(t' - \frac{T_i}{2} - \sum_{k=0}^{i-1} T_k) + 1(t' - T_i - \sum_{k=0}^{i-1} T_k) \right] \quad (11)$$

where  $1(t)$  is the Heaviside's step function and  $T_k$  is the time width of the  $k$ -th step in the modulation waveform.

Taking into account that

$$T_1 + T_2 + \dots + T_N = T_0 \quad (12)$$

one can write (9) in the form

$$u(t) \approx \text{Re} \left\{ e^{j\omega t} \int_0^L \rho(z) \delta n(z) \left[ \sum_{i=1}^N \frac{T_i}{T_0} \cos\left(i\omega_s \cdot \frac{z}{v_g}\right) \cdot e^{-2jk_0 z} \right] dz \right\}. \quad (13)$$

The summation term in (13) represents the SCF  $\gamma(z)$ . For the sake of generalization we can introduce the phase shift  $\zeta_i = (i \cdot \omega_s / v_g) \cdot z_\xi$  into (13) that can be generated by the phase shifter as it was mentioned above. For  $\gamma(z)$  we can now write a more general relation

$$\gamma(z) = \sum_{i=0}^N t_i \cos\left(i\omega_s \cdot \frac{z}{v_g} - \zeta_i\right) = \sum_{i=0}^N t_i \cos\left(i\omega_s \cdot \frac{z - z_{xi}}{v_g}\right) \quad (14)$$

where  $t_0$  represents the magnitude of DC component in the periodic coherence function. From the experimental point of view  $t_0$  is equal to the relative time at the early stages of the frequency modulation waveform when no changes of frequency take place.

For the case when the frequency and phase modulation waveforms are composed of a set of symmetrical and equally long steps ( $T_i = T_0/N$ ), as it is depicted in Fig. 3, the SCF (14) can be transformed into the closed form

$$\gamma(z) = \sum_{i=1}^N \frac{T_i}{T_0} \cos\left(i\omega_s \cdot \frac{z - z_\xi}{v_g}\right) = \frac{\cos\left[(N+1) \cdot \frac{\omega_s}{2} \cdot \frac{z - z_\xi}{v_g}\right]}{N \sin\left[\frac{\omega_s}{2} \cdot \frac{z - z_\xi}{v_g}\right]}. \quad (15)$$

The graphs of this function (first two peaks), shifted by  $z_\xi = 0.05$  m with respect to  $z = 0$ , for three frequencies  $f_s = 800, 1000$  and  $1600$  MHz,  $N = 64$  and  $v_g = 2 \times 10^8$  m/s are drawn in Fig. 4a. Figure 4b manifests the possibility for the first peak scanning through the phase shift when the separation frequency is constant  $f_s = 800$  MHz.

### 2. The triangle and square shape of the SCF

An important field of application of various modifications of OTDR represent fiber optic sensors, especially those with distributed parameters [14]. Recently [15] besides the  $\delta$ -like SCF also other SCF shapes find application mainly in sensors with distributed parameters. For illustration we present here the modulation waveforms for triangle and square shape SCFs. They are described by

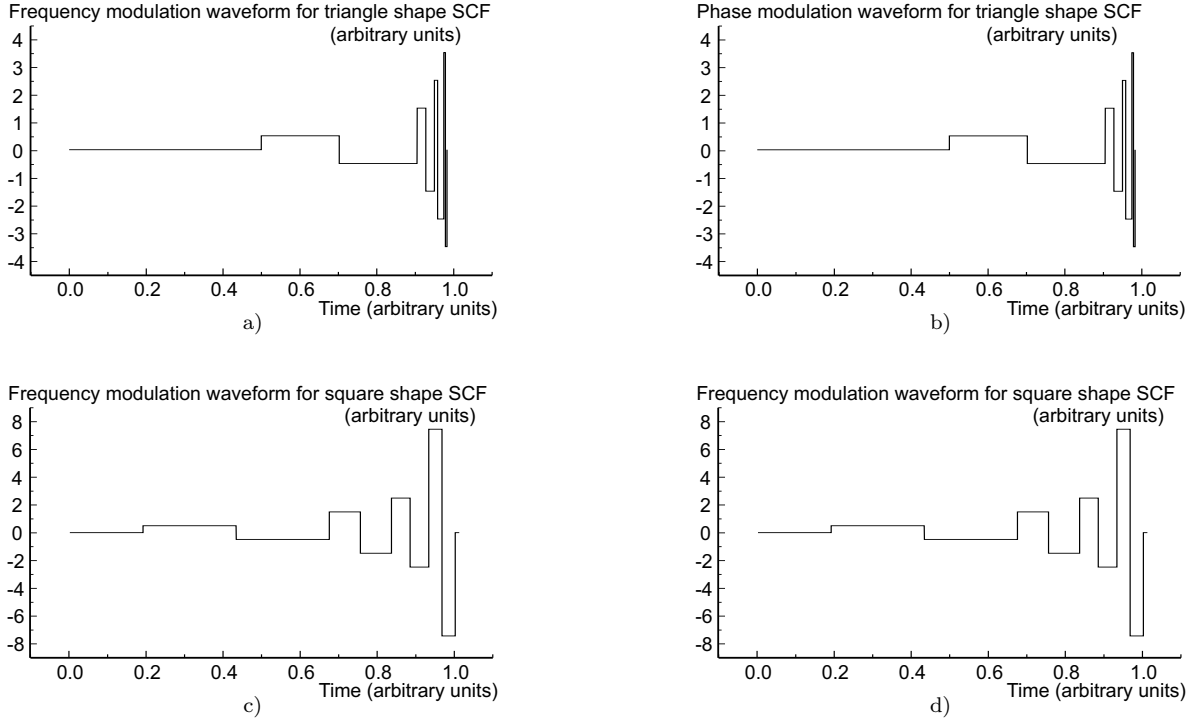


**Fig. 5.** The schematic illustration of the frequency and phase modulation waveforms for the triangle (a, b) and square shape SCF (c, d)

the well-known Fourier series

$$\gamma_{\text{tr}}(z) = 0.5 + \frac{4}{\pi^2} \left[ \frac{1}{1^2} \cos \frac{\omega_s}{2v_g} z + \frac{1}{3^2} \cos \frac{3\omega_s}{2v_g} z + \frac{1}{5^2} \cos \frac{5\omega_s}{2v_g} z + \dots \right] \quad (16)$$

$$\gamma_{\text{sq}}(z) = 0.5 + \frac{4}{\pi} \left[ \cos \frac{\omega_s}{2v_g} z - \frac{1}{3} \cos \frac{3\omega_s}{2v_g} z + \frac{1}{5} \cos \frac{5\omega_s}{2v_g} z - \dots \right]. \quad (17)$$

For these functions we have quite a different situation due to the appearance of the dc component and due to the fact that only odd multiples of the separation frequency exist. Moreover, they change the signs in the case of  $\gamma_{\text{sq}}$ . As a consequence the width of the corresponding steps in the modulation waveform will be decreasing and the change of the sign at some terms has to be reflected by introducing a phase shift of  $\pi$  at proper time periods. The corresponding frequency and phase modulation functions are outlined schematically in Figs. 5a–d.

For the modulation waveforms in pictures (a) and (b) the scanning of the SCF peak through the phase shift is proposed while for the case in pictures (c) and (d) only scanning through the separation frequency  $f_s$  is expected. The phase modulation waveform in (d) assures only the change of sign at appropriate terms in Fourier series, see (15).

#### 4 BASIC PROPERTIES OF THE OCDR–SCF

The most significant advantage of the OCDR–SCF consists in straightforward obtaining of the measurement

results without any complex calculation as it is the case at other methods. The second significant fact is that the experimental apparatus does not include any moving parts such as scanned mirrors or so. The scanning of the peak of the  $\delta$ -like CF can be achieved by changing the magnitude of the separation frequency  $f_s$  in the frequency modulation waveform. However, it brings some difficulties. First, it does not allow measurements in the vicinity of  $z = 0$  and, second, the space resolution as we show below does depend on the frequency  $f_s$ , which means that the space resolution changes along the fiber. Another way how to scan the CF peak is the use of phase shift as it was mentioned in the previous section. It is very easy for realization and it does not suffer from any similar drawbacks as it is in the case of scanning by changing  $f_s$ . The measurement by this method is much faster as compared with other known methods. The measurement time within one period of the modulation waveform takes roughly several tens of  $\mu\text{s}$  [16].

The sensitivity and consequently the dynamical range of the method is determined mostly by the heterodyne detection scheme. The sensitivity achieved can be better than  $-130$  dBm. Moreover, the method does not suffer from the dead zone caused by strong Fresnel reflections. They are eliminated by the narrow coherence function. The dynamical range of measurement by this method is limited mainly by the existence of coherence function sub-peaks.

The space resolution is determined by the full width at half maximum (FWHM) of the main peak of the coherence function. It can be derived from relation (13) and

is approximately given by the relation

$$\Delta z_{\text{res}} = \frac{v_g}{N f_g}. \quad (18)$$

The period of the peaks defines the measurement range, that is defined by

$$\Delta z_{\text{range}} = \frac{v_g}{f_g}. \quad (19)$$

The space resolution increases with the increasing number of steps in one period of the frequency modulation waveform and the separation frequency of the first step in the modulation waveform. In the contrary, the measurement range is defined only by the separation frequency in the first step of the modulation waveform.

From the experimental point of view the most significant problems concern the non-linearity between the injection current amplitude and the optical frequency of the laser diode and the frequency response to the modulation waveform (transients). Both factors can be compensated by predistortion of the current modulation waveform and by the use of special optical filters and optical gratings [17].

## 5 CONCLUSIONS

The OADR-SCF seems to become a significant tool for testing of optical components and networks. Among the existing optical reflectometric methods it is difficult to find the method that could be comparable with OADR-SCF as for the speed of measurement and straightforward obtaining of results. This method does not use any mechanical moving components and there is no need for numerical processing of the measured signals. Contemporary laser diodes allow to synthesize the  $\delta$ -like CF that gives the space resolution of a few mm. The space resolution of the method is inversely proportional to the tunable range of the laser diode. One can expect that the use of broadly tunable lasers will improve the space resolution to sub-millimeter range. Recently also other shapes of SCF like triangle or square shape find use in applications of sensors with distributed parameters.

## Acknowledgement

This work was supported by VEGA Grant 1/7603/20.

## REFERENCES

- [1] BARNOSKI, K.—JENSEN, S. M.: Fiber Waveguide: a Novel Technique for Investigating Attenuation Characteristics, *Appl. Opt.* **15** No. 9 (1976), 2112–2115.
- [2] ZOBOLI, M.—BASSI, P.: High Spatial Resolution Attenuation Measurements by a Correlation Technique, *Appl. Opt.* **22** No. 23 (1983), 3680–3681.
- [3] NAZARATHY, M.—NEWTON, S. A.—GIFFARD, R. P.—MOBERLY, D. S.—SISCHKA, W. R.—TRUTNA, Jr.—FOSTER, S.: Real Time Long-Range Complementary Correlation Optical Time-Domain Reflectometer, *J. Lightwave Tech.* **7** No. 1 (1989), 24–38.
- [4] KING, P. J. *et al*: Development of a Coherent OTDR Instrument, *J. Lightwave Tech.* **5** No. 4 (1987), 616–623.
- [5] ČERMAK, O.—JASENEK, J.: The Principles and Application of the Photon-Counting Method in the OTDR, *J. Electrical Engineering* **44** No. 12 (1993), 367–372.
- [6] TAKADA, K.—TAKATO, N.—NODA, J.—NOGUCHI, Y.: Characterization of Silica Based Waveguides with an Interferometric Optical Time-Domain Reflectometry System Using a 1.3- $\mu\text{m}$ -wavelength superluminescent diode, *Opt. Lett.* **14** (1989), 706–708.
- [7] WEID, J. P.—PASSY, R.—MUSSI, G.—GISIN, N.: On the Characterization of Optical Fiber Network Components with Optical Frequency Domain Reflectometry, *J. Lightwave Tech.* **15** No. 7 (1997), 1131–41.
- [8] NAZARATHY, M.—DOLFI, D. V.: Optical Synchronous Detection with Coded Modulation Applied to Frequency Domain Reflectometry, *Tech. Dig. of OFC 1989, THF3*, 1989, p. 150.
- [9] HOTATE, SAIDA, K.: Distributed Fiber-Optic Stress Sensor by Synthesis of the Optical Coherence Function, *IEEE Photonics Technology Letters* **9** No. 4 (1997), 484–486.
- [10] YOUNQUIST, R. C.—CARR, S.—DAVIES, D. E. N.: Optical Coherence-Domain Reflectometry: A New Optical Evaluation Technique, *Opt. Lett.* **12** No. 3 (1987), 158–160.
- [11] BORN, M.—WOLF, E.: *Principles of Optics*, Pergamon Press, 1968.
- [12] NAKAZAWA: Rayleigh Backscattering Theory for Single-Mode Optical Fibers, *Opt. Soc. Am.* **73** No. 9 (1983), 1175–1179.
- [13] HOTATE, K.—SAIDA, T.: Phase-Modulating Optical Coherence Domain Reflectometry by Synthesis of Coherence Function, *Electronics Letters* **31** No. 6 (1995), 475–476.
- [14] TURÁN, J.—PETRÍK, S.: *Fiber Optic sensors*, Alfa, Bratislava, 1991. (in Slovak)
- [15] HOTATE, K.—SONG, X.—HE, Z.: Stress-Location Measurements Along an Optical Fiber by Synthesis of Triangle-Shaped Optical Coherence Function, *IEEE Photonics Technol. Lett.*
- [16] HOTATE, K.—SAIDA, T.: High Resolution Reflectometry for Diagnosis of Optical Devices by Synthesis of Coherence Function, *Tech. Digest Symp. on OF Meas. 1998, NIST*, Boulder, Colorado, USA, pp. 91–96.
- [17] KAMATANI, O.—HOTATE, K.: Optical Coherence Domain Reflectometry by Synthesis of Coherence Function with Nonlinearity Compensation in Frequency Modulation of a Laser Diode, *J. Lightwave Tech.* **11** No. 11 (1993), 1854–1862.

Received 8 October 2001

**Jozef Jasenek** (Doc, Ing, PhD), born in 1947, Bobrov (Northern Slovakia), graduated from the Faculty of Electrical Engineering and Information Technology of the Slovak University of Technology Bratislava in 1971, in solid state physics, PhD studies completed in 1980. Appointed Associate Professor for Electromagnetic field theory in 1986. During the years 1994 - 2000 he served as a vice-dean responsible for the pedagogical affairs. His professional interests concern the development and application of microwave ferrite materials for microwave circuit components design and the theory of linear and nonlinear optical waveguides and in the development of experimental methods for the testing of optical waveguides and optical fiber two-port components. He is involved in analysis and implementation of optical reflectometric methods (OTDR and its modifications). He was leading several scientific grants and has published more than 40 scientific papers in journals or presented in scientific conferences at home and abroad.